

## Surface Modification of Multiwalled Carbon Nanotubes via Gliding Arc Plasma for the Reinforcement of Polypropylene

Z. Luo,<sup>1</sup> X. Cai,<sup>1</sup> R. Y. Hong,<sup>1,2</sup> J. H. Li,<sup>3</sup> D. G. Wei,<sup>4</sup> G. H. Luo,<sup>5</sup> H. Z. Li<sup>2</sup>

<sup>1</sup>College of Chemistry, Chemical Engineering and Materials Science and Key Laboratory of Organic Synthesis of Jiangsu Province, Soochow University, SIP, Suzhou 215123, China

<sup>2</sup>State Key Laboratory of Multiphase Complex Systems, Institute of Process Engineering, Chinese Academy of Sciences, Beijing 100080, China

<sup>3</sup>Tangshan Zhongrun Coal Chemical Company Ltd., Seaport Economic Development Zone, Tangshan 063611, China

<sup>4</sup>Center for Nanoscale Systems, School of Engineering and Applied Science, Harvard University, Cambridge, Massachusetts 02139

<sup>5</sup>Department of Chemical Engineering, Tsinghua University, Beijing 100084, China

Correspondence to: R. Y. Hong (E-mail: rhong@suda.edu.cn)

**ABSTRACT:** To increase the applicability of multiwalled carbon nanotubes (MWCNTs), functional groups were generated on the generally inert surface of MWCNTs using gliding arc (GA) plasma. MWCNTs were modified using plasma polymerization with styrene (St) as monomer. The surface compositional and structural changes that occur on MWCNTs were investigated using FT-IR, Raman spectroscopy, BET surface area, and elemental analysis. Dispersion of the treated MWCNTs in different solvents was evaluated. Transmission electron microscopy images showed that the plasma-treated MWCNTs had a better dispersion than the untreated ones in nonpolar solvents. Subsequently, MWCNTs-reinforced polypropylene (PP) composites were prepared by internal batch mixing with the addition of 1.0 wt % MWCNTs. The morphology of MWCNTs/PP nanocomposites was studied through scanning electron microscopy. Observations of SEM images showed that the plasma-treated MWCNTs had a better dispersion than the untreated MWCNTs either on the composite fracture surfaces or inside the PP matrix. Moreover, the mechanical tests showed that the tensile strength and elongation at break were improved with the addition of polystyrene-grafted MWCNTs. © 2012 Wiley Periodicals, Inc. *J. Appl. Polym. Sci.* 000: 000–000, 2012

**KEYWORDS:** multiwalled carbon nanotubes; gliding arc; plasma; nanocomposites

Received 13 March 2010; accepted 8 March 2012; published online

DOI: 10.1002/app.37986

### INTRODUCTION

Carbon nanotubes (CNTs), discovered in 1952<sup>1</sup> by Radushkevich, have become of keen interest to material scientists. Iijima initiated the current worldwide intensive research on CNTs by publishing his findings in 1991.<sup>2</sup> CNTs exhibit specific physical and chemical properties due to their unique hollow structures consisting of concentric graphite cylinders and have many potential applications in mechanical reinforcement, electron transport, energy storage, and so on.<sup>2–4</sup> Because of their unique properties, CNTs have attracted considerable attention in the last few years. CNTs have been considered as an ideal filler for polymer composites due to their outstanding mechanical,<sup>5–7</sup> electrical,<sup>8–11</sup> and thermal properties,<sup>12</sup> as well as their high aspect ratio. As far as the practical applications of CNTs are concerned, it has been proven that the incorporation of CNTs into

polymers is a simple and effective method to improve the mechanical and thermal properties of polymers.<sup>13–16</sup> Tang et al.<sup>17</sup> reported their effort to improve the tensile properties of chitosan using both CNTs and clay simultaneously.

However, CNTs are subject to be agglomerated, resulting in poor dispersion in polymer matrix that limits their practical applications in polymer composites. To obviously improve the properties of polymers with the addition of CNTs, two main issues should be resolved: homogeneous dispersion of CNTs in polymer matrix and strong interfacial interaction between the two phases. In this regard, a key issue in development of polymer/CNTs composites is how to maximize the compatibility between CNTs and polymer matrix.<sup>18–20</sup> Proper surface treatment can make the CNTs surface easily be wetted by the matrix (hence reducing voids, flaws, and cracks), and the CNTs can be

© 2012 Wiley Periodicals, Inc.

intertwisted with polymer matrix by covalent bond. This improves both the uniformity of the bonding and mechanical properties of the composites.<sup>21</sup> Therefore, surface treatment and good dispersion of CNTs are required in industrial applications.<sup>22</sup> Surface treatment of the CNTs may roughly be classified into two categories: chemical treatment by oxidizing acids and (dry) plasma-chemical treatment.<sup>23</sup> Chemical oxidation and amine treatment are included in the first category. The CNTs are opened at the end and the terminal carbons are converted to carboxylic acids by oxidation in concentrated sulfuric and nitric acids.

The second category includes gas plasma treatment. Since the 1960s, plasma technology has quickly evolved into a valuable technique to engineer surface properties without alteration of the bulk composition<sup>24,25</sup> and is nowadays widely used in various applications such as plasma cleaning, plasma sterilization, plasma coatings, and fluorination.<sup>26</sup> In comparison with conventional liquid or gaseous chemical reagents, on the one hand, plasma constitutes a very little explored medium for the surface treatment of materials. Because of the nonequilibrium and non-isothermal behavior of glow discharge plasma, these ionized gases can lead to novel results when used as treatment media for CNTs.<sup>27</sup> On the other hand, plasma is used to modify CNTs<sup>28</sup> in a facile and environmentally sound manner, avoiding the discerning conditions as well as a comparatively high consumption and accompanying wastage of chemicals wet chemical methods require.<sup>29</sup> In addition, plasma treatments are classified into two categories according to different gas atmospheres present: nonpolymerizable gas and polymerizable monomer gas. The use of nonpolymerizable plasma gas (air, Ar, He, O<sub>2</sub>, and N<sub>2</sub>) to modify the substrate surface in terms of functionalization and etching, especially plasma functionalization and generation of surface-bound functional groups without deposition of a coating, is considered a promising solution to enhance the reactivity of a substrate surface.<sup>29</sup> For example, Park and Cho<sup>30</sup> studied the influence of oxygen plasma treatment on the surface and adsorption properties of carbon blacks and reported that oxygen plasma treatment generated oxygen-containing functional groups, such as, carboxyl, hydroxyl, lactone, and carbonyl groups, on the carbon black surfaces, resulting in a decrease in the equilibrium spreading pressure or London dispersive component of surface free energy. On the other hand, polymerizable monomer gases (ethylene, styrene, acrylic acid, and butadiene) have been effectively used to modify CNT surfaces, leading to significantly improved dispersion in the polymer matrix.<sup>31</sup> The main principle of plasma polymerization technique is that the ionized and excited molecules and radicals which created by the electrical field bombard can react with the surface of the substrate. These activated molecules may etch, sputter, or deposit on the substrate surface. Avila-Orta et al.<sup>32</sup> have deposited a PPEG ultrathin polymer coating (thickness 1–3 nm) on the surfaces of multiwall and aligned carbon nanotubes by means of a plasma polymerization treatment.

Polypropylene (PP) is a well-known thermoplastic and is commercially available in different grades with different types of additives. It is a nonpolar semicrystalline polymer with low surface tension. The thermoplastic PP matrix was selected because thermoplastics are now receiving increasing interest due to their

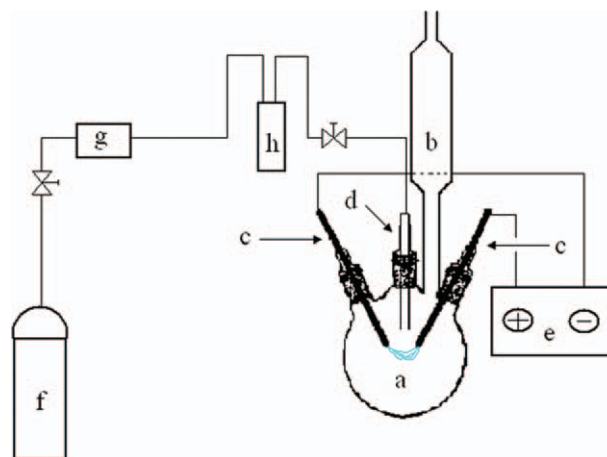


**Figure 1.** Designed apparatus for plasma processing (a) four mouth flask, (b) custom-built fluidized bed reactor, (c) electrodes, (d) nozzle, (e) power source, (f) argon gas cylinder, (g) monomer tank, and (h) surge tank. [Color figure can be viewed in the online issue, which is available at [wileyonlinelibrary.com](http://wileyonlinelibrary.com).]

manufacturing versatility, low price, high strength, and stiffness.<sup>33</sup> The recyclability of thermoplastics gives it an advantage, because subsequent processing is to be used in this study (pelletizing, extrusion, and rheological evaluation).

The aim of the present work is to study the surface properties such as wettability, dispersability, surface functional groups, specific surface area of MWCNTs treated by gliding arc plasma, and the effect of this treatment on the dispersion and tensile properties of MWCNTs/PP nanocomposites.

## EXPERIMENTAL

### Materials

The multiwalled carbon nanotubes (MWCNTs) used in this study was supplied by CNano Technology (Beijing). The MWCNTs synthesized by chemical vapor deposition (CVD) have the average diameter of 10 nm with purity over 95%, and were used as received. The styrene (St) monomer to graft the MWCNTs was purchased from Sinopharm chemical Reagent, which was distilled under reduced pressure prior to use. The PP in which the MWCNTs were cast was supplied by Nanjing Yangzi Petrochemical Project. Carrier gas argon (Ar) was of chemical grade (at a purity of 99%).

### Preparation of Polystyrene-Grafted MWCNTs by Plasma Treatment

In this study, the MWCNTs were grafted with PS using plasma polymerization of styrene monomer. The atmospheric plasma polymerization was carried out in a designed reactor. Figure 1 shows a schematic representation of the plasma reactor, designed by authors, used for the plasma polymerization described in this work. It consists of four main parts: (1) the reaction chamber includes four mouth flask (250 mL) and a custom-built fluidized bed reactor (length = 40 cm), (2) two cylindrical electrodes which are made of stainless steel (diameter = 5 mm) and separated at a distance of 2 cm, (3) a power



**Figure 2.** Photographs of MWCNTs treated by different plasma flame (a) air, (b) argon, and (c) styrene (argon is used as carrier gas). [Color figure can be viewed in the online issue, which is available at [wileyonlinelibrary.com](http://wileyonlinelibrary.com).]

source of high frequency and voltage is used for generating plasma, (4) a monomer tank and carrier gas cylinder.

The mixture of monomer (styrene) and carrier gas (argon) was driven into the reactor (a) to circulate the MWCNTs through a magnetic bar and mass flow controllers. The surface of the MWCNTs was continuously renewed and exposed to the plasma for polymer deposition during the plasma polymerization. The GA plasma generator (100 W, 20 kHz) and the mixture of monomer and carrier gas flow rate (7.5 L/min) were applied for 30 min at atmospheric pressure to produce the plasma polystyrene (PS).

#### Preparation of the MWCNTs/PP Nanocomposites

PP was dried in a vacuum oven at 80°C for 24 h. MWCNTs/PP nanocomposites were prepared by melt mixing in SU-70B internal batch mixer at 200°C with a rotor speed of 60 rpm. Blending was carried out by feeding PP and MWCNTs into the mixer. After mixing for 5 min, the mixture was then extruded and pressed by XLB-400 × 400 × 2 plate vulcanization machines at 200°C, and cooled to ambient temperature. The MWCNTs/PP nanocomposites were prepared containing 1 wt % untreated and PS grafted MWCNTs.

#### Characterization

FT-IR (Nicolet FT-IR Avatar 460 analyzer with the KBr method) was used to characterize PS on the MWCNTs and was employed from 500 to 4000  $\text{cm}^{-1}$  at room temperature. For TEM measurements of the plasma-treated MWCNTs, the MWCNTs were suspended in toluene and water in turn, and were drop cast onto a carbon-coated copper grid followed by solvent evaporation in air at room temperature. All of the TEM images were obtained using Hitachi H-600-II field emission transmission electron microscopy (TEM) at an acceleration voltage of 200 kV. The element analysis of untreated and plasma treated MWCNTs was conducted using a Hitachi S-4700 scanning electron microscope apparatus (SEM-EDS). X-ray spectrum elements analysis range is Be-92U, accuracy is 129.25 eV. The untreated and PS-grafted MWCNTs were tested for dispersion in two solvents with different polarity indexes: water and toluene. After standing for 2 h, photographs were taken to evaluate the degree of dispersion. Raman analysis was performed with an XY multichannel Raman microspectrometer (JY-HR800) employing continuous wave lasers of 514.53 nm (green) and 633 nm (red) wavelengths. The laser spot size was  $\leq 1 \mu\text{m}$ ,

spectral resolution 1  $\text{cm}^{-1}$ , spectra were measured in the 100–4000  $\text{cm}^{-1}$  range. The surface of the MWCNTs was characterized by physical adsorption tests. This was done by exposing the MWCNTs to flowing  $\text{N}_2$  at 77 K in an automated adsorption apparatus (Quantachrome ASIMP). The measure range is 0.01–3000  $\text{m}^2/\text{g}$  for BET and 3.5–5000 Å for pore size distribution, respectively. A Hitachi S-4700 scanning electron microscope (SEM) with 15.0 kV beam voltage was used to observe the fractured surface of MWCNTs/PP nanocomposites. The tensile tests of MWCNTs/PP nanocomposites were performed according to the China National Standards, GB/T 14,452-93 using a universal testing machine (WDT20, Shenzhen KQL Testing Instruments) at room temperature. A PC was connected to the testing machine, and the crosshead speed was set to be 2 mm/min. The force transducer with a precision of  $\pm 0.02\%$  was provided by Transcell Tech. (USA). The GB standards were established according to the ISO ones.

## RESULTS AND DISCUSSION

### Different Plasma Atmospheres Analysis

Figure 2(a–c) shows the various colors of plasma flame generated using air, argon, and styrene as working gas, respectively. There is an obvious difference in color between nonmonomer

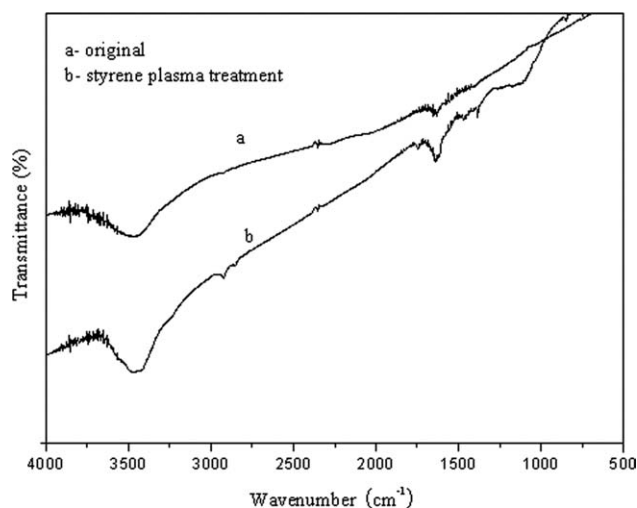


**Figure 3.** FTIR spectra of untreated and PS-grafted MWCNTs (a) untreated MWCNTs and (b) PS-grafted MWCNTs.

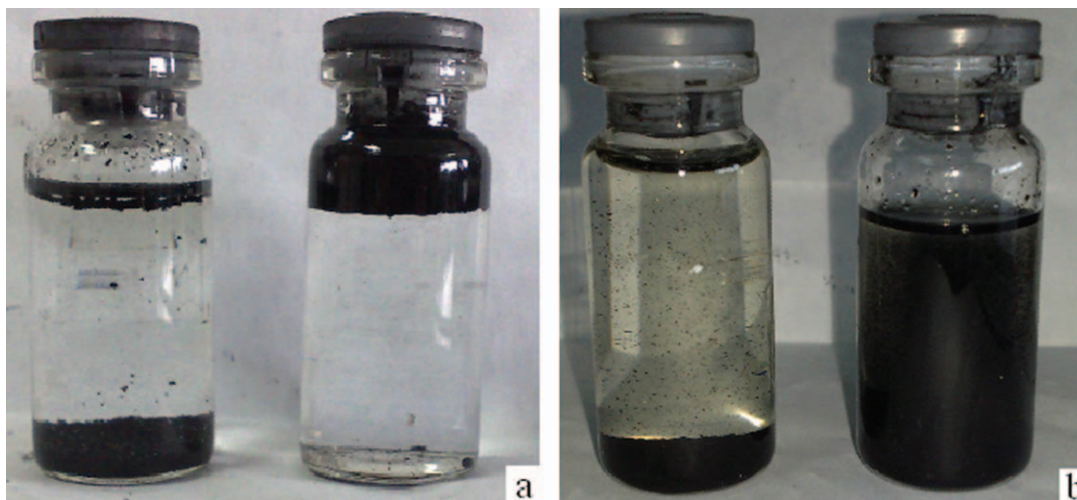


**Figure 4.** Dispersion of the untreated and PS-grafted MWCNTs in water (a) and toluene (b).

gas (air, argon) and monomer gas (styrene). The brightness of the argon plasma flame is greater than that of air plasma flame because the argon can be easily ionized and inert, and hence argon is used as carrier gas. It is then seen that the greenish appearance of the discharge is due to the C<sub>2</sub> band emission around 515 nm, which is different from nonmonomer gas, as shown in Figure 2(c). Initiating polymerization of styrene monomer by plasma is believed to be by creation of the active centers at the surface of substrate.<sup>34</sup> It is speculated that gaseous monomer molecules can diffuse through the bulk of the substrate, more easily if it is already powdery, and polymerized at any location on the surface randomly. Styrene plasma depositions resulted in the formation of PS on the MWCNTs surface. However, plasma polymerizations can also take place in the gas phase (leading to dusty plasmas)—diffusion into the bulk is slow and would only apply to the monomer.

#### FT-IR Analysis

FT-IR was carried out to study the chemistry of the surface on the MWCNTs. Figure 3 shows the FT-IR spectrum of the untreated and PS grafted MWCNTs. The FT-IR spectrum of the sample obtained by PS graft reveals some changes in relation to the original sample consisting in appearance of the band near 1400, 1600, and 2900  $\text{cm}^{-1}$ . Those bands have been identified as the C—C vibrating absorption of the benzene ring and C—H stretching of methyl. Therefore, one can conclude that styrene plasma treatments can produce coating of PS on the surface of MWCNTs.

#### Dispersion Test

Dispersion tests give a fair idea whether a treatment on the MWCNTs has been achieved or not. Figure 4(a) presents a photograph of two vials containing untreated and PS-grafted

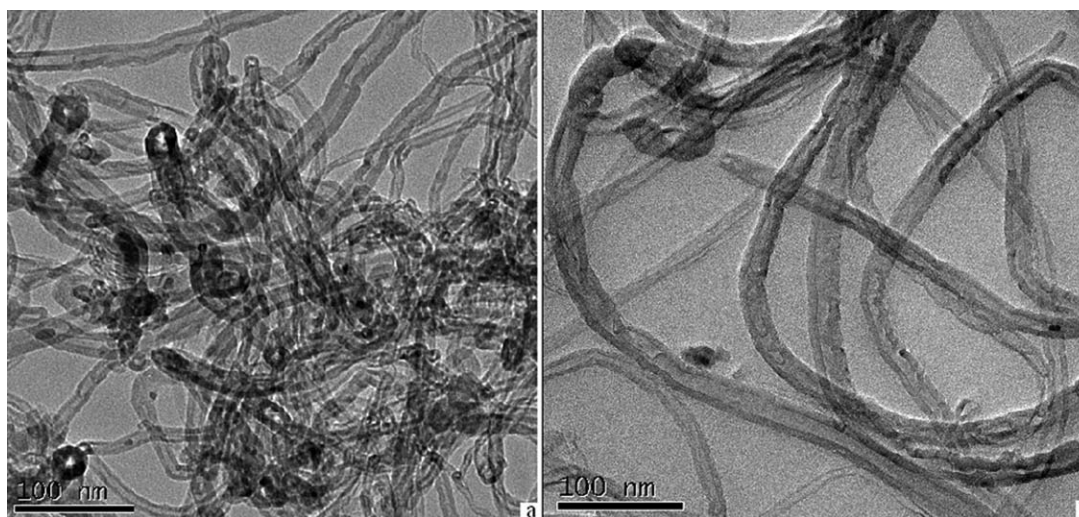


**Figure 5.** TEM image of the MWCNTs: (a) untreated MWCNTs and (b) PS-grafted MWCNTs dispersion in toluene.

**Table I.** SEM-EDS Analysis of Different MWCNTs

Sample	C element wt %	O element wt %	Other element wt %
Untreated	94.62	4.50	0.88
Argon plasma treated	89.08	2.04	8.78
PS grafted	95.86	3.42	0.72

MWCNTs dispersed in water. The untreated MWCNTs sedimented almost immediately in a high polarity solvent such as water, but the treated ones (for 30 min, 100 W) floated on the water after standing for 48 h, suggesting complete rejection between high polar solvent and nonpolar PS coating of the treated ones. In addition, a photograph of another two vials containing untreated and PS-grafted MWCNTs dispersed in toluene is shown in Figure 4(b). The untreated MWCNTs sedimented in nonpolar solvent such as toluene, but the treated samples fairly dispersed in the toluene solvent because of a strong interaction between the nonpolar solvent and PS coating of the treated MWCNTs. The dispersion test clearly indicates the hydrophobic character of the PS coating due to the presence of the benzene ring and methyl groups determined by FTIR.

Figure 5 shows the TEM image of the untreated and PS-grafted MWCNTs in toluene after sonication (5 min). It is found that the untreated MWCNTs have more tangled organization and poor dispersibility, as shown in Figure 5(a,b) shows that the PS-grafted MWCNTs, after plasma-induced grafting polymerization, have a less-tangled organization, which demonstrates that the grafted styrene molecule efficiently promotes the dispersal of the MWCNTs.

### Elemental Analysis

SEM-EDS can be used for the analysis of element contents of MWCNTs measured at several locations. Table I shows SEM-EDS element analysis of the untreated and plasma-treated MWCNTs, and it is found that the content of C and O element of the untreated MWCNTs is 94.62 and 4.50%, respectively. In contrast, the presence of PS coating on the surface of MWCNTs was confirmed by elemental analysis, which revealed an increase of the C content from 94.62 to 95.86% and decrease of the O content from 4.5 to 3.42%. On the other hand, the content of C and O element decreases to 89.08 and 2.04% by argon plasma treatment, respectively, since the oxygen-containing groups on the surface of MWCNTs were removed by argon plasma.

### Raman Microprobe Spectrometry

Confocal Raman microprobe spectrometry can be used as a tool for the surface characterization of partially ordered carbon materials, with an estimated analysis depth of 700–1500 nm. It is expected to introduce some degree of surface disorder with plasma treatment, which can be measured by Raman spectrometry. For all studied samples, it can be found that there are two relatively broad bands centered at  $1580\text{ cm}^{-1}$  (G band, typical of graphitic order) and  $1320\text{ cm}^{-1}$  (D bands, typical of structural disorder and defects) of first order spectrum. The ratio of the peak height at  $1320\text{ cm}^{-1}$  to that at  $1580\text{ cm}^{-1}$  ( $I_D/I_G$ ) always can be used for evaluating the degree of graphitization,

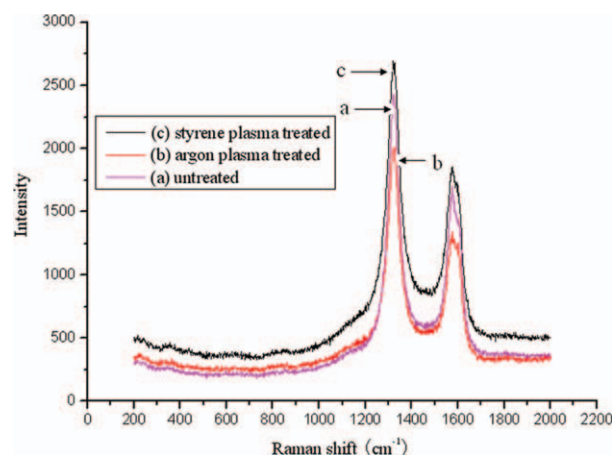


**Figure 6.** Raman spectra of (a) untreated, (b) argon plasma treated, and (c) PS-grafted MWCNTs. [Color figure can be viewed in the online issue, which is available at [wileyonlinelibrary.com](http://wileyonlinelibrary.com).]

because a large  $I_D/I_G$  value indicates a highly disordered carbon microstructure. The second order Raman envelope was very weak, typical for disordered carbons.<sup>35,36</sup> From Figure 6, it is found that the Raman spectra of both the untreated and plasma-treated MWCNTs have first order spectra. It can also be found that intensity ratios of D band to G band ( $I_D/I_G$ ) parameters change somewhat after plasma treatment. The surfaces of the plasma-treated MWCNTs had a disordered structure, since the  $I_D/I_G$  value for the argon plasma treated and PS grafted is 1.4886 and 1.4418, respectively, higher than that of the untreated sample (1.431). The  $I_D/I_G$  value is increased, because argon gas etched the carbon surface and the carbon atoms of MWCNTs participated in reaction, many  $sp^2$  hybrid carbon atoms turn into  $sp^3$  hybrid carbon atoms in styrene plasma polymerization process. Therefore, Ar plasma should lead to  $sp^3$  hybridization due to etching process, PS grafted should lead to  $sp^3$  and  $sp^2$ , untreated MWCNTs should mainly have  $sp^2$ .

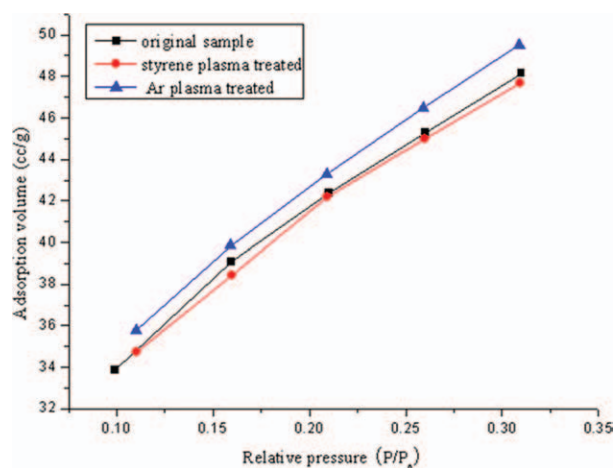


**Figure 7.** Dependence of  $N_2$  volume adsorbed by MWCNTs at 77 K on the relative pressure. [Color figure can be viewed in the online issue, which is available at [wileyonlinelibrary.com](http://wileyonlinelibrary.com).]

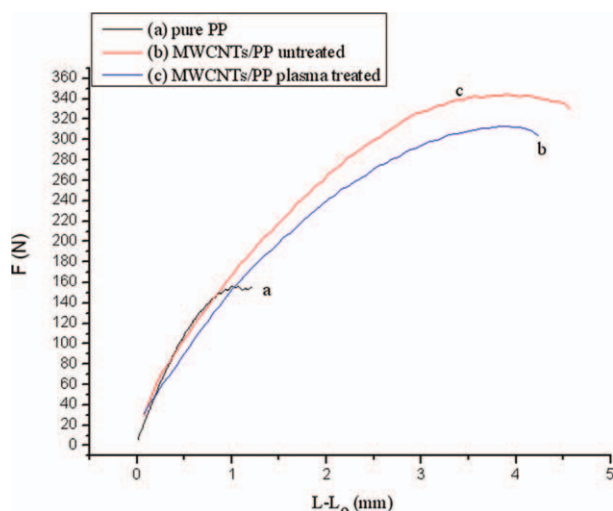


**Figure 8.** Tensile stress–strain of pure PP (a), and PP composites with untreated (b) and PS grafted (c) 1 wt % MWCNTs. [Color figure can be viewed in the online issue, which is available at [wileyonlinelibrary.com](http://wileyonlinelibrary.com).]

### Adsorption Properties

Figure 7 shows the adsorption isotherms of the MWCNTs before and after plasma treatment. From the BET adsorption isotherms, the specific surface areas ( $S_{\text{BET}}$ ) can be calculated according to the method presented in literature.<sup>37</sup>

It is found that the  $S_{\text{BET}}$  of the samples grafted by PS (147.8  $\text{m}^2/\text{g}$ ) systematically decreased, while the  $S_{\text{BET}}$  of the samples treated by argon plasma (153.9  $\text{m}^2/\text{g}$ ) is higher than that of the untreated MWCNTs (149.4  $\text{m}^2/\text{g}$ ). From the above results, one can easily conclude that treated by the styrene plasma atmosphere, a very thin PS coating is formed on the surface of MWCNTs and hence a small decrease in the original absorptive capacity. For the argon plasma, the increase in absorptive capacity is due to the etching of nonpolymerizable plasma on the surface of MWCNTs.

**Table II.** Mechanical Properties of Pure PP and MWCNTs/PP Composites

Fillers	Tensile strength (MPa)	Young's modulus (GPa)	Elongation at break (%)
No filler	15.67	1.359	1.20
Untreated MWCNTs	31.32	1.339	3.04
PS-grafted MWCNTs	34.42	1.357	3.29

### Tensile Properties of MWCNTs/PP Nanocomposites

Tensile test is the most widely used method to evaluate the reinforcing effect of MWCNTs into PP. Measurement is performed five times for each sample. Figure 8 shows stress–strain curve of pure PP and nanocomposites containing MWCNTs and the mechanical parameters were listed in Table II. It is found that the tensile strength and elongation at break of surface modified MWCNTs/PP composites are higher than those of untreated MWCNTs/PP composites and pure PP. It is attributed to the functional groups which are formed on the CNT surface can improve the compatibility between the MWCNTs and PP and improve the mechanical property of polymer. There are functional groups bonding on the CNT surface, so the PP chains can easily be fixed onto MWCNTs by covalent bond in melt mixing, resulting in a strong interfacial interaction between MWCNTs and PP.<sup>38</sup> The interfacial bonding enables an effective stress transfer between the polymer and the CNTs. Generally, composites with PS-grafted MWCNTs have higher tensile strength than those with untreated ones. The tensile strength of PP reinforced by 1.0 wt % modified MWCNTs increased up to 34.42 MPa. This indicates, in turn, that the PS-grafted MWCNTs can well-dispersed in PP matrix, resulting in improvement in tensile property.

The fracture surface obtained through the tensile tests of the MWCNTs/PP composites is observed by the SEM. As show in Figure 9, nonuniform agglomerates can be seen from the fracture surfaces of the PP composites loaded with the untreated MWCNTs. Besides, some MWCNTs are seen completely loose,

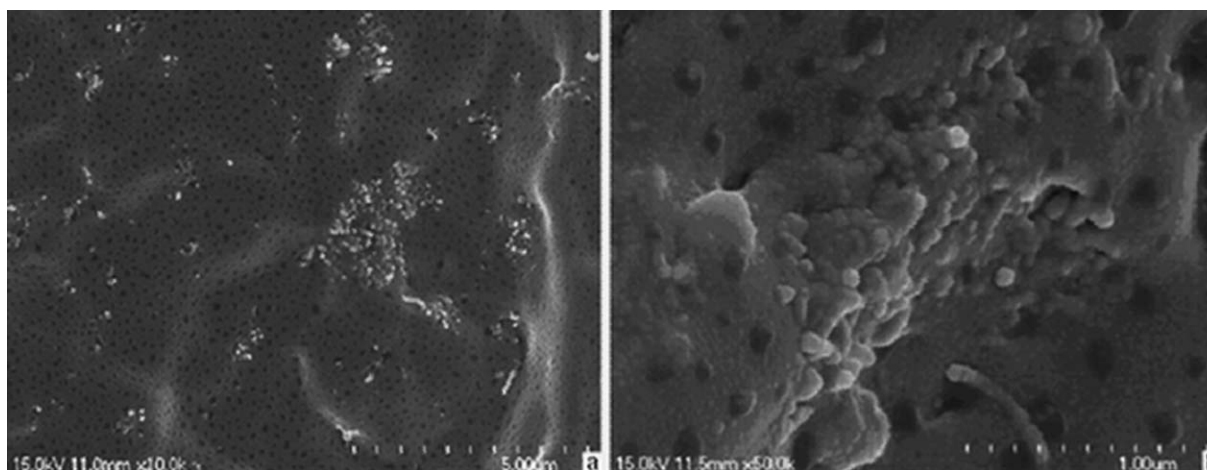


**Figure 9.** SEM images of the fracture surface in composites containing 1 wt % of untreated MWCNTs (a)  $\times 10,000$  and (b)  $\times 50,000$  (The white spots indicate MWCNTs.).

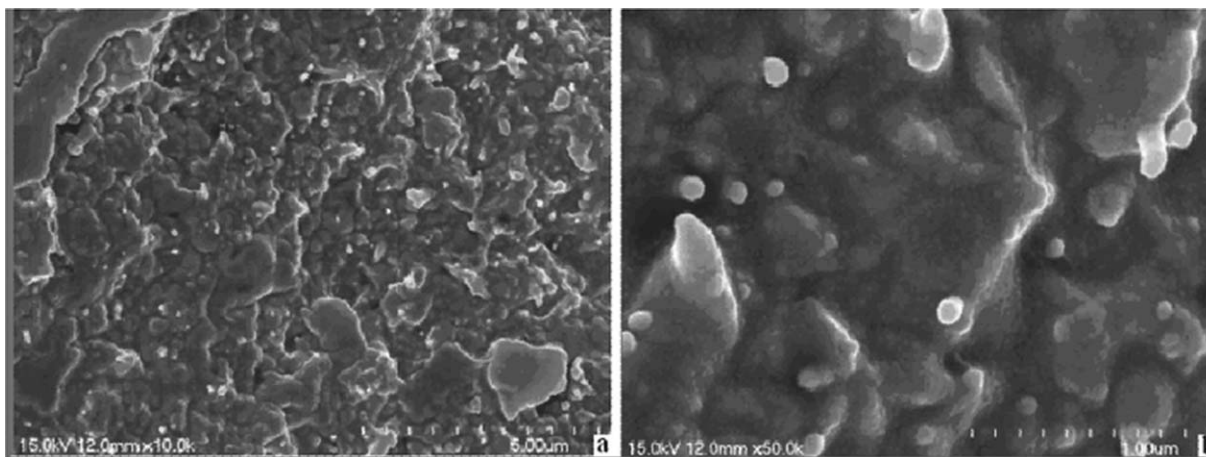


**Figure 10.** SEM images of the fracture surface in composites containing 1 wt % of PS-grafted MWCNTs (a)  $\times 10,000$  and (b)  $\times 50,000$  (The white spots indicate MWCNTs).

without any attachment to the PP matrix. Many holes observed in Figure 9 are formed by pulling out of nanotubes from the PP matrix during the tensile test. It also shows that the untreated MWCNTs have poor attachment to the PP matrix. The white regions in Figure 9(a) represent the aggregated MWCNTs and the region is magnified as shown in Figure 9(b) to verify the existence of MWCNTs.

It can be found that PS-grafted MWCNTs are dispersed well in PP matrix, as shown in Figure 10(a). Moreover, PS-grafted MWCNTs are not pulled out, because the polymer coatings and active groups formed by the plasma treatment contribute to good dispersion and strong interfacial bonding. In the magnified image as shown in Figure 10(b), a number of broken bundles are found, demonstrating that strong interfacial bonding exists between the PP matrix and the functionalized nanotubes.

## CONCLUSIONS

A PS coating was deposited on the surface of MWCNTs by means of a gliding arc plasma process. There were hydrophobic groups on the surface of PS-grafted MWCNTs which could be confirmed by FTIR and dispersion test. The PS-grafted MWCNTs exhibited a very stable dispersion in nonpolar solvents and a poor dispersion in high polar solvents, which indicated that the surface of PS-grafted MWCNTs is hydrophobic. SEM-EDS, BET, and Raman spectrometry results suggested the change of surface structure and elemental composition.

The MWCNTs/PP nanocomposites could be prepared by melt mixing with the addition of 1.0 wt % nanotubes. The SEM results showed that the PS-grafted MWCNTs nanocomposites had a good dispersion of nanotubes inside the polymer matrix, leading to an improvement in mechanical properties. The composites containing the PS-grafted MWCNTs exhibited higher tensile strength and elongation at break than that with the untreated MWCNTs, because the surface treatments provided more homogeneous dispersion of MWCNTs and stronger interaction between the MWCNTs and the polymer matrix. Therefore, the plasma-treated MWCNTs might be a very promising reinforcement filler in polymers and other matrices to pro-

duce composite materials with superior physical properties in some high-demanding engineering applications.

## ACKNOWLEDGMENTS

The project was supported by the National Natural Science Foundation of China (NSFC; Nos. 20876100 and 20736004), the National Basic Research Program of China (973 Program, No. 2009CB219904), the Key Lab. of Organic Synthesis of Jiangsu Prov., National Post-doctoral Science Foundation (20090451176), the Commission of Science and Technology of Suzhou Municipality (Nos. YJS0917, SG0978), Technology Innovation Foundation of Suzhou New District and MOST (11C26223204581), Natural Science Foundation of Jiangsu Prov. (BK2011328) and Minjiang Scholarship of Fujian Prov.

## REFERENCES

1. Monthieux, M.; Kuznetsov, V. L. *Carbon* **2006**, *44*, 1621.
2. Baughman, R. H.; Zakhidov, A. A.; deHeer, W. A. *Science* **2002**, *297*, 787.
3. Tomanek, D.; Enbody, R. J. *Science and application of nanotubes*. Kluwer Academic Publishers: New York, **2000**.
4. Vigolo, B.; Coulon, C.; Maugey, M.; Zakri, C.; Poulin, P. *Science* **2005**, *309*, 920.
5. Wong, E. W.; Sheehan, P. E.; Lieber, C. M. *Science* **1997**, *277*, 1971.
6. Yu, M.; Lourie, O.; Dyer, M. J.; Kelly, T. F.; Ruoff, R. S. *Science* **2000**, *287*, 637.
7. Ou, C. F.; Shiu, M. C. *J. Appl. Polym. Sci.* **2010**, *115*, 2648.
8. Ramasubramaniam, R.; Chen, J.; Liu, H. *Appl. Phys. Lett.* **2003**, *83*, 2928.
9. Kim, B.; Lee, J.; Yu, I. *J. Appl. Phys.* **2003**, *94*, 6724.
10. Kilbride, B. E.; Coleman, J.; Fraysse, N. J.; Fournet, P.; Cadek, M.; Drury, A. *J. Appl. Phys.* **2002**, *92*, 4024.
11. Grossiord, N.; Loos, J.; Regev, O.; Koning, C. E. *Chem. Mater.* **2006**, *18*, 1089.

12. Biercuk, M. J.; Llaguno, M. C.; Radosavljevic, M.; Hyun, J. K.; Johnson, A. T.; Fischer, J. E. *Appl. Phys. Lett.* **2002**, *80*, 2767.
13. Thostenson, E. T.; Li, C. Y.; Chou, T. W. *Compos. Sci. Technol.* **2005**, *65*, 491.
14. Du, F.; Fischer, J. E.; Winey, K. I. *Phys. Re B* **2005**, *72*, 121404.
15. Bryning, M. B.; Islam, M. F.; Kikkawa, J. M.; Yodh, A. G. *Adv. Mater.* **2005**, *17*, 1186.
16. Bouhelal, S.; Cagiao, M. E.; Khellaf, S.; Tabet, H.; Djellouli, B.; Benachour, D.; Balta Calleja, F. J. *J. Appl. Polym. Sci.* **2010**, *115*, 2645.
17. Tang, C. Y.; Xiang, L. X.; Su, J. X.; Wang, K.; Yang, C. Y.; Zhang, Q.; Fu, Q. *J. Phys. Chem. B* **2008**, *112*, 3876.
18. Coleman, J. N.; Khan, U.; Blau, W. J.; Gun'ko, Y. K. *Carbon* **2006**, *44*, 1624.
19. Moniruzzaman, M.; Winey, K. I. *Macromolecules* **2006**, *39*, 5194.
20. Coleman, J. N.; Khan, U.; Blau, W. J.; Gun'ko, Y. K. *Adv. Mater.* **2006**, *18*, 689.
21. Dilsiz, N.; Erinc, N. K.; Bayramli, E.; Akovali, G. *Carbon* **1995**, *33*, 853.
22. Kim, J. A.; Seong, D. G.; Kang, T. J.; Youn, J. R. *Carbon* **2006**, *44*, 1898.
23. Chen, J.; Rao, A. M.; Lyuksyutov, S.; Mikhail, E. *J. Phys. Chem. B* **2001**, *105*, 2525.
24. Morita, S.; Hattori, S. *Applications of plasma polymers*. Academic Press: Boston, **1990**, 423 p.
25. Yasuda, H. *Plasma Polymerization*; Academic Press: London, **1985**, 344 p.
26. d'Agostino, R.; Favia, P.; Oehr, C.; Wertheimer, M. R. *Plasma Process Polym.* **2005**, *2*, 7.
27. Cascarini de torre, L. E.; Bottani, E. J.; Martinez-alonso, A.; Cuesta, A.; Garcia, A. B.; Tascon, J. M. D. *Carbon* **1998**, *36*, 277.
28. Vohrer, U.; Zschoerper, N. P.; Koehne, Y.; Langowski, S.; Oehr, C. *Plasma Process Polym.* **2007**, *4*, 871.
29. Zschoerper, N. P.; Katzenmaier, V.; Vohrer, U.; Haupt, M.; Oehr, C.; Hirth, T. *Carbon* **2009**, *47*, 2174.
30. Park, S. J.; Cho, K. S.; Ryu, S. K. *Carbon* **2003**, *41*, 1437.
31. Shi, D.; Lian, J.; He, P.; Wang, L. M.; Xiao, F.; Yang, L. *Appl. Phys. Lett.* **2003**, *83*, 5301.
32. Avila-Ortaa, C. A.; Cruz-Delgado, V. J.; Neira-Velazqueza, M. G.; Hernandez-Hernandez, E.; Mendez-Padilla, M. G.; Medellin-Rodriguez, F. J. *Carbon* **2009**, *47*, 1916.
33. Lozano, K.; Barrera, E. V. *J. Appl. Polym. Sci.* **2001**, *79*, 125.
34. Inagaki, N.; Yasuda, H. *J. Appl. Polym. Sci.* **1981**, *26*, 3557.
35. Boudou, J. P.; Paredes, J. I.; Cuesta, A.; Martinez-Alonso, A.; Tascon, J. M. D. *Carbon* **2003**, *41*, 41.
36. Cuesta, A.; Dhamelin-court, P.; Laureyns, J.; Martinez-Alonso, A.; Tascon, J. M. D. *Carbon* **1994**, *32*, 1523.
37. Sing, K. S. W.; Everett, D. H.; Haul, R. A. W.; Moscou, L.; Pierotti, R. A.; Rouquerol, J. R. *Pure Appl. Chem.* **1985**, *57*, 603.
38. Fu, H. P.; Hong, R. Y.; Zhang, Y. J.; Li, H. Z.; Xu, B.; Zheng, Y.; Wei, D. G. *Polym. Adv. Technol.* **2009**, *20*, 84.